Journal of Pharmaceutical Innovation
https://doi.org/10.1007/s12247-020-09450-4

ORIGINAL ARTICLE

Implications of Solid Lipid Nanoparticles of Ganoderic Acid for the Treatment and Management of Hepatocellular Carcinoma

Mahfoozur Rahman[1] · Sarwar Beg[2] · Khalid S. Alharbi[3] · Nabil K. Alruwaili[4] · Nasser Hadal Alotaibi[5] · Abdulaziz I. Alzarea[5] · Waleed H. Almalki[6] · Sattam Khulaif Alenezi[7] · Waleed M. Altowayan[8] · Mohammed S. Alshammari[9] · Muhammad Afzal[3] · Shakir Saleem[10] · Vikas Kumar[11]

Abstract

Purpose The present work describes the systematic development of ganoderic acid (GA)–loaded solid lipid nanoparticles (SLNs) for the treatment of hepatocellular carcinoma (HCC).

Methods A full factorial design was employed for optimization of the GA-loaded SLNs prepared by hot-homogenization method, where Capmul MCMC10 and soy lecithin were used as solid lipid and surfactant, while poloxamer 188 was used as stabilizer. GA-SLNs were subjected to detailed in vitro and in vivo characterization studies.

Results The optimized GA-SLNs exhibited particle size of 73 nm, entrapment efficiency of 66% and loading capacity of 11.53%. In vitro drug release study carried out by microdialysis bag method indicated more than 70% drug release was observed within the 8-h time period. In vitro cytotoxicity study of GA-SLNs performed on HepG2 cell line by MTT assay indicated that GA-SLNs exhibited comparatively higher cytotoxicity than GA solution and Blank SLNs. IC_{50} values of GA-SLNs and GA solution after 72 h exposure were found to be 25.1 μg/mL and 36.2 μg/mL, respectively. Moreover, particle size and amount of GA entrapped in SLNs exhibited nonsignificant difference over a 12-week storage period at 25 °C/75% RH. In vivo anticancer activity of GA-SLNs in male Wistar rats demonstrated significant reduction ($P < 0.001$) in the size of hepatic nodules and variation in the levels of oxidative stress in a dose-dependent manner.

Conclusions Overall, GA-SLNs showed better chemoprotective effect over GA solution, thus construed superior efficacy of the developed nanoformulation for the treatment of HCC.

Keywords Ganoderic acid · Solid lipid nanoparticles · Experimental design · Hepatoprotective · Antioxidant

Electronic supplementary material The online version of this article (https://doi.org/10.1007/s12247-020-09450-4) contains supplementary material, which is available to authorized users.

✉ Vikas Kumar
phvikas@gmail.com

[1] Department of Pharmaceutical Sciences, Faculty of Health Sciences, Sam Higginbottom University of Agriculture, Technology and Sciences, Allahabad, UP, India

[2] Department of Pharmaceutics, School of Pharmaceutical Education and Research, Jamia Hamdard, New Delhi, India

[3] Department of Pharmacology, College of Pharmacy, Jouf University, Sakakah, Saudi Arabia

[4] Department of Pharmaceutics, College of Pharmacy, Jouf University, Sakakah, Saudi Arabia

[5] Department of Clinical Pharmacy, College of Pharmacy, Jouf University, Sakakah, Saudi Arabia

[6] Department of Pharmacology and Toxicology, College of Pharmacy, Umm Al-Qura University, Makkah, Saudi Arabia

[7] Department of Pharmacology and Toxicology, Unaizah College of Pharmacy, Qassim University, Qassim, Saudi Arabia

[8] Department of Pharmacy Practice, College of Pharmacy, Qassim University, Qassim, Saudi Arabia

[9] Department of Pharmacy Practice, Unaizah College of Pharmacy, Qassim University, Qassim, Saudi Arabia

[10] Department of Pharmacology, Chitkara College of Pharmacy, Chitkara University, Rajpura, Punjab, India

[11] Natural Product Drug Discovery Laboratory, Faculty of Health Sciences, Sam Higginbottom University of Agriculture, Technology & Sciences, Allahabad, UP, India

Published online: 30 May 2020

Introduction

Liver cancer is a major health problem across the globe and also considered as the fifth most vulnerable cause of death due to cancers worldwide. Among the various types of liver tumours, hepatocellular carcinoma (HCC) is the most frequently occurring form [1]. Over 620,000 cases are reported worldwide each year with 80% of cases from Africa, South East Asia and China [2, 3]. There is only a limited therapeutic strategy available for the treatment of HCC, which includes surgical resection and hepatic transplantation marked with moderate success rates when detected under early stage of diagnosis in the patients by imaging and high-throughput techniques [4]. Other treatment approaches like hormone therapy, radiotherapy and chemotherapy are available but only provide symptomatic relief with no satisfactory solution. Hence, there is need for comprehensive understanding of the biological basis of hepatic malignancy, and it might suggest new strategies for effective treatment [5].

Diethyl-nitrosamine (DEN) is prominently found in beverages, agriculture chemicals and tobacco products and it is the most important environmental carcinogen which causes HCC. Further, DEN is involved in the disruption of nuclear enzymes responsible for DNA replication/repair, and repeated exposure of this to animal induces HCC [6]. The mechanistic studies indicate that overproduction of reactive oxygen species (ROS) plays a key role in the aetiology of HCC. ROS is a radical (or O2) superoxides (O2*), hydroxyl, peroxyl or alkoxyl radical species, e.g. unpaired electron oxygen. ROS occurs in physiologically based living cells. Oxidative phosphorylation is the main cause of ROS and can be produced to a small part by the action of other proteins (e.g. five-lipoxygenase, cyclooxygenase, xanthine oxidase), cytochrome P450 or cell-component auto-oxidation [6].

The overproduction of ROS due to metabolic biotransformation of DEN leads to oxidative stress which damages the DNA, proteins and lipids to result in oxidative damage via change in gene expression and intracellular signalling pathways paving the way for the generation of HCC [6]. Generation of oxidative stress may lead to alteration of lipid peroxidation (LPO) and production of oxidative products including crotonaldehyde, acrolein, 4-hydroxy 2-neonatal (HNE) and malondialdehyde (MDA); thus, DEN is considered as a strong hepatocellular carcinogen [7]. The available chemotherapy is not sufficient for optimum therapeutic benefits and associated with several serious adverse effects [8].

To overcome such problems, naturally occurring biotherapeutics have gained wider importance in liver diseases. From centuries, the medicinal mushrooms entitled as *Ganoderma lucidum* have been used for the treatment of liver ailments. It is a medicinal mushroom forming white rot fungus [9]. Ganoderic acid (GA) is an active constituent found in it and is the most important active pharmacological constituent of *G. lucidum* [9]. Furthermore, it shows beneficial effect against the free radicals and reduces cell damage induced by the mutagens. Some of the studies have reported its mechanism of action as hepatoprotective agent and immunity enhancer for producing strong antioxidant action [9, 10]. Notwithstanding its therapeutic benefits, the delivery of GA is quite challenging due to biopharmaceutical issues. This requires suitable drug carriers which can be used for effective drug delivery to achieve maximal therapeutic benefits.

Solid lipid nanoparticles (SLNs) are the most interesting carriers for oral drug delivery application due to their excellent biocompatibility, high drug loading capacity, long-term stability and feasibility for large-scale production [11]. Moreover, various researchers have reported enhanced intracellular drug delivery of the anticancer drugs when administered using SLNs [11]. SLNs are the colloidal system primarily composed of solid lipids. These have gained high importance in the delivery of various poorly soluble drugs including anticancer drug [11]. Despite immense drug delivery benefits, the idea of rationally designing nanoformulations like SLNs is highly critical, as minor variations in the formulation composition and process parameters greatly influence the end-product quality and performance. Lately, the concept of systematic development using Quality by Design paradigm was documented in ICH Q8 guideline and endorsed by USFDA, EMA, MHRA and several other regulatory agencies across the globe for attaining consistency in the quality of pharmaceutical products [12–15]. Nevertheless, the concept has now been percolated in nanopharmaceutical product development too, which not only provides science and risk-based understanding but also ensures quality without failure. Some of the research works reported by our group is a testimony of it [16–21].

With respect to the research work carried out in literature for improving the biopharmaceutical performance of GA using the nanocarriers, the specialized formulations like the GA-NLCs by our research group in previous report [22] and GA-SLNs by other researchers [23]. Although said formulations showed a definitive improvement in the biopharmaceutical attributes of the drug, yet the present study was undertaken to describe the key findings of the GA-SLNs systematically optimized using the experimental design for improving the efficacy of drug therapy against DEN-induced HCC in rats.

Material and Methods

Chemicals

Ganoderic acid (GA) and DEN were purchased from Sigma-Aldrich, USA. Solid lipids (i.e. Capmul MCM C10 and lecithin soy) were obtained from Gattefosse, Cedex, France. Poloxamers (Kolliphor® P 188, Kolliphor® P 338 and

Kolliphor® P 407) were obtained from BASF, Mumbai, India. Tween 80 was purchased from Fischer Scientific Pvt. Ltd., India. HPLC grade solvents were procured from local vendors. Diethyl-nitrosamine (DEN) was procured from Sigma-Aldrich (USA), respectively. Human hepatocellular carcinoma cell line (HepG2; ATCC HB-8065) was generously provided by National Center for Cell Science, Pune, Maharashtra, India, for the present research work. Dulbecco's modified Eagle's medium (DMEM) and foetal bovine serum (FBS) were supplied by Himedia Chemical Pvt. Ltd., Mumbai, India.

Analytical Method Development

The chromatographic separation of ganoderic acid was performed using reversed-phase high performance liquid chromatography (HPLC) method. Agilent 1260 Infinity HPLC system fitted with a Zorbax C18 column and isocratic elution of mobile phase containing mixture of solvents (solvent A, water + 0.1% acetic acid; solvent B, acetonitrile) was employed for method development. The detection wavelength was set at 252 nm at a flow rate of 0.4 mL/min. The run time was kept at 15 min and peak areas were noted. The linearity range of the developed method was evaluated and validated for accuracy, precision, robustness, limit of quantification (LOQ) and limit of detection (LOD).

Preparation of the GA-SLNs

The GA-SLNs were prepared by hot-homogenization and solvent diffusion method as reported in literature reports with suitable modifications [22–24]. The range of amount of solid lipid used for preparing the SLNs was selected on the basis of solubility study. In this regard, Capmul MCMC10 (i.e. 150 to 400 mg) and soy lecithin (30 to 80 mg) were selected as the solid lipid and cosurfactant, and both were heated up to 70 °C. A fixed quantity of the drug (i.e. 50 mg) was added with keep gentle mixing for complete solubilization in the lipidic phase. Further, 5% w/v of aqueous solution of poloxamer 188 was prepared in 10 mL of distilled water at 70 °C [19]. Then, aqueous phase was incorporated into the organic phase under constant homogenization at the speed of 6000–10,000 rpm for 2 to 6 min to get a uniform dispersion. In addition, excess water (10 mL) was applied to solvents and subsequently constantly stirred at 1000–2500 rpm for 1–4 h in the ice bath condition for the acquisition of SLNs and further the obtained formulation stored at 4 °C in the refrigerator [19].

Optimization of SLNs by Experimental Design Approach

A full factorial design was employed for systemic optimization of the SLNs, where various formulation parameters viz. concentrations of the solid lipid (i.e. Capmul MCMC10), surfactant (i.e. poloxamer 188) and cosurfactant (i.e. soy lecithin), while formulation parameters like homogenization speed and stirring speed were taken as the factors. SLNs were prepared and evaluated for various critical quality attributes (CQAs) like particle size, entrapment efficiency and drug loading capacity. Design Expert® 9.0 software was used for analysis of experimental data. Second-order polynomial model was used for optimization data which included terms for both main effect and interaction effect. The fitness model was assessed through analysis of the statistical parameters such as P value, impact ratio (r^2), and prediction residual curves. Surface response assessment was conducted to understand the connection between the characteristics of the formulations investigated. Numerical optimization and desired feature, accompanied by the delimitation of the optimum formula in the development room, were chosen for the optimal product. Validation of optimization methodology was carried out by preparing the check-point formulations, and comparing the values obtained between the predicted and observed values of the CQAs of GA-SLNs.

Characterization of the GA-SLNs

Particle Size

Dynamic light dispersion technique with Zetasizer ZS 90 was used to measure the particle size (PS) distribution of SLNs prepared in accordance with the experiential design (M/s Malvern Instruments, Worcestershire, UK).

Entrapment Efficiency and Drug Loading Capacity

Entrapment efficiency (EE) and drug loading capacity (LC) are the parameters which provide the proportion of drug effectively entrapped in the SLNs. It was calculated by micro dialysis technique as per the reported method [8, 22]. Briefly, a SLN dispersion aliquot (2 mL) was centrifuged at 10,000 rpm (5590g), where both the supernatant phase and the pellet formed in the bottom of centrifuge tube were collected. From the supernatant phase containing the unentrapped drug, an aliquot (100 μL) sample was taken, then suitably diluted and filtered for subsequent analysis. Similarly, the pellet containing SLNs was also digested in 0.1% w/v solution of ethanol and ultrasonicated at 9 mV amplitude for 15 min for complete removal of the drug. Then, the drug was extracted in the mobile phase, suitably filtered and quantified by HPLC. Equations 1 and 2 are used for encapsulation efficiency and loading capacity.

$$\mathrm{EE}\% = \frac{\text{Total quantity of GA} - \text{Free quantity of GA}}{\text{Total Quantity of GA}} \times 100 \quad (1)$$

$$\text{LC}\ (\%) = \frac{\text{Total amount of GA encapsulated in SLN}}{\text{Total amount of SLN weight}} \times 100 \quad (2)$$

Transmission Electron Microscopy

Aliquot (1 mL) of the SLNs were diluted 100 times with sterile triple distilled water and stained with 1% solution of phosphotungstic acid on a copper grid. The sample was allowed to dry on grid and further visualized under the transmission electron microscope (JEM-2100F, M/s Jeol, Tokyo, Japan).

Field Emission Scanning Electron Microscopy

Field emission scanning electron microscopy (FE-SEM) uses the photon absorption layer of the conductor, which has a strong tungsten needle (diameter point 10–100 nm) inside the microscope tube. It works at an accelerating voltage between 0.5 and 30 kV (~ 10–6 Pa). A drop of diluted SLN sample was placed on a Nucleopore Track-Etch membrane, which is then dried inside a heat chamber and coated with a platinum sputter. Finally, the images were taken at − 140 °C using FE-SEM SEM at 15KV voltage (SU-8010 Ultra-high-resolution Cold emission, Hitachi, Japan).

In Vitro Drug Release Study

In vitro drug release study was performed for evaluating the release profile of the SLNs in of 250 mL simulated intestinal fluid (pH 6.8) at 100 rpm and 37 ± 0.5 °C temperature for 24 h. The formulations were filled in the dialysis bag with molecular cut-off weight of 12 Da (M/s Himedia limited, Mumbai, India). SLN dispersion equivalent to 50 mg of drug was filled in the dialysis bag and subject to study. Aliquot (0.5 mL) of samples were taken periodically and filled with the same quantity of fresh medium maintained at 37 ± 0.5 °C. The samples were analyzed by HPLC and cumulative % drug release was calculated. The obtained drug release data was fitted with various mathematical models such as zero-order, first-order, Higuchi and Korsmeyer-Peppas to evaluate the release kinetic on the basis of comparison of the values of correlation coefficient (R). Also, the mechanism of drug release from the SLNs was evaluated using release exponent (n) obtained from the Korsmeyer-Peppas equation [22].

Cell Culture and Cell Viability Study

Human hepatocellular carcinoma cell line (HepG2) was grown using Dulbecco's modified Eagle's medium (DMEM) along with 10% (v/v) foetal bovine serum (FBS), 1 mM L-glutamine, 100 U/ml penicillin and 100 mg/ml streptomycin. Further, the cells were kept at the 37 °C and 5% CO_2/95% air environment for performing 3-[4, 5-dimethylthiazol-2-yl]-2,5-diphenyltetrazolium bromide (MTT) assay to determine the cytotoxicity of GA-SLNs on HePG2 cell line [22]. In short, the cell line was seeded using the moisturized incubator with ganoderic acid (10–60 μg/ml) in the 96-well plates for 24, 48 and 72 h at 37 °C. Following incubation in the phosphate buffer saline, MTT (10 μL) solution was then added to all plates and again incubated for 2 h at 37 °C. The optical density was also determined by ELISA reader (BioTek, USA) at 570 nm and the cell viability was calculated.

$$\%\text{cell inhibition} = 100 - \left\{\frac{\text{Test}}{\text{Control}}\right\} \times 100 \quad (3)$$

In order to determine half maximum inhibitory concentration (IC_{50}), the GraphPad Prism software was used.

Sterilization and Stability Studies

The optimized GA-SLNs were subjected to sterilization by filtration. The SLN dispersions were passed through a 0.22-μm membrane filter for sterile filtration [25]. Binderfi KBF-240 climate chamber was used for (Binder GmbHfi Ltd., Munchen, Germany) evaluating the stability of the optimized SLN [26]. The stability studies were conducted at 25 °C/60% RH and 40 °C/75% RH. The formulations were packed in the vials, tightly sealed and subjected to stability studies for 0, 1, 2, 4, 8 and 12 weeks. The formulations were evaluated for parameters like PS, PDI, EE and LC at periodic time intervals.

Animal Study

Male Albino Wistar strain rats of weight 150 to 200 g were taken for the proposed experimental study and were acclimatized under at 25 ± 2 °C; 12-/12-h light and dark cycle. The animals were provided with standard rat diet and water ad libitum. Experiments were conducted as per the guidelines issued by all the international guidances as well as the guidelines of Committee for Protection, Control and Supervision on Experimental Animals (CPCSEA), Govt. of India. The study protocol was approved by the Institutional Animal Ethical Committee (IAEC) of Siddhartha Institute of Pharmacy, Dehradun, India (Reg. No. SIP/IAEC/PCOL/06/2017). In addition, all laboratory parameters linked to animals were performed in accordance with the appropriate IAEC rules and laws.

Induction of HCC

The rats were given a single intraperitoneal injection of DEN dissolved in the phosphate buffer saline (200 mg/kg), except

the animals in the control group. The animals were examined after 10 days for the formation of tumours.

Experimental Procedure

The rats were categorized into 6 groups, with six animals in each group. Animals in group 1 (naïve) were considered as the control group and received 0.9% w/v of normal saline 5 mL/kg/day p.o. Single dose (200 mg/kg) of DEN was administered to animals in group II (DEN control), while animals in group III (DEN control) were provided with 5 mL/kg/day p.o. single dose of GA (25 mg/kg) for 14 weeks. Animals in group IV (DEN control) received a single dose of GA (100 mg/kg) of 5 mL/kg/day p.o. for 14 weeks, group V DEN control treated GA-SLN (25 mg/kg) single dose 5 mL/kg/day p.o. treated for 14 weeks.GA (100 mg/kg) 5 mL/kg/day p.o. treated in the group VI for 14 weeks. At periodic intervals, the body weight of all rats was measured. The rats were euthanized by cervical dislocation at the end of the experimental study and approximately 0.5 mL blood samples were withdrawn from the retroorbital plexus in the heparinized vials and stored at 4 °C until further use. The blood samples were centrifuged at 5000 rpm at 37 °C and serum was collected for estimation of various antioxidant parameters such as lipoxygenase (LPO), catalase (CAT), superoxide dismutase (SOD), glutathione peroxidase (GPx) and glutathione-S-transferase (GST) [27, 28]. Moreover, the liver tissues were restored under formalin for the histopathological examination.

Data Analysis

All the experimental data were subjected to one-way ANOVA, followed by Dunnet's test for post hoc analysis at 5% level of significance.

Results and Discussion

Analytical Method Development

The reversed-phase HPLC method developed using isocratic solvent system showed retention of GA at 8.7 min with linearity in the drug concentration ranging between 15 and 40 ng/mL, limit of quantification of 12 ng/mL and limit of detection of 5 ng/mL, respectively.

Selection of the Ingredients

From the equilibrium solubility studies of GA, the solubility in various lipids was found to be in the following order: Capmul MCM C10>Compritol 888>GMS>Stearic acid. Therefore, Capmul MCM C10 was selected as the lipid for formulation development. The equilibrium solubility of drug in surfactants and cosurfactants was found to be in the order of poloxamer 188>Tween 80>Unitop100 and lecithin soy>Phospholipid 90G (PL90G)>Phospholipid 90H (PL90H). Therefore, Capmul MCMC10, poloxamer 188 and lecithin soy were selected as the key ingredients for the formulation development of SLNs.

Systematic Optimization of the GA-SLNs

The second-order quadratic polynomial model was selected for the optimization data, which is shown in Eq. 4. Analysis of polynomial coefficients revealed the existence of interactions among the studied factors on the CQAs. Further, the evaluation of model fitting using parameters revealed correlation coefficient (R) ranging between 0.963 and 0.996, and insignificant lack of fit ($P > 0.05$), indicated aptness of the selected model and excellent goodness of fit of the experimental data (Supplementary data Table 1).

$$Y = \beta 0 + \beta 1X1 + \beta 2X2 + \beta 3X3 + \beta 4X1X2 + \beta 5X2X3 \quad (4)$$

where Y = response variables; β0 = intercept; β1 to β3 = coefficients of linear model terms; β4 to β5 = coefficients of linear interaction terms; and X1, X2, X3 = three factors chosen for experimental design based optimization.

The 3D-response surface and 2D-contour plots depicted in Supplementary data Figures 1-3 reveals the cause–effect relationship among the studied factors on the response variables of SLNs. Supplementary data Figures 1A to 1B portrays the influence of Capmul MCM C10 (A) and poloxamer (B) on the particle size. Increase in Capmul MCM C10 indicates a sharp rising trend on the values of particle size, while poloxamer has no influence on particle size. Minimum particle size was observed at high levels of Capmul MCM C10 and poloxamer. Supplementary data Figure 2A to 2B depicts the influence of poloxamer (B) and lecithin (C) on the entrapment efficiency. The effect of poloxamer on entrapment efficiency is quite negligible, while increase in lecithin content shows a mild positive effect on entrapment efficiency. High lecithin and poloxamer concentrations revealed high values of the entrapment efficiency. Supplementary data Figure 3A to 3B portrays the effect of Capmul MCM C10 (A) and poloxamer (B) on the drug loading potential. Capmul MCM C10 exhibited positive influence on the drug loading potential, while poloxamer has not shown any significant influence on the drug loading efficiency.

Characterization of the GA-SLNs

Supplementary data Table 1 represents the values of the CQA (like as particle size, entrapment efficiency and loading

capacity) for the SLN formulations prepared as per the experimental design.

Particle Size Determination

The particle size of GA-SLNs was found to be ranging between 60 and 100 nm, which shows the nanostructured nature of the formulation. Smaller particle size, however, was obtained at the medium levels of lipids, surfactants, cosurfactants and high level of homogenization speed and stirring speed, and vice versa.

Entrapment Efficiency and Drug Loading Capacity

The developed formulations showed high entrapment efficiency ranging between 45 and 81%, and drug loading capacity of 8 to 15.2%. Maximum entrapment efficiency and loading capacity was observed in formulations containing intermediate levels of the lipid and surfactant, and high level of the stirring speed [8, 22].

Search for the Optimal Formulation and Validation

The optimized formulation was identified by trading-off various CQAs to achieve desired objectives by minimization of the particle size, and maximization of the entrapment efficiency and loading capacity for improved biopharmaceutical performance. Based on the aforementioned objectives, the selection criteria were embarked upon for locating the optimized formulation with the particle size less than 100 nm, encapsulation efficiency > 60% and loading capacity > 11%, as provided during the numerical optimization in order to identify the optimized formulation with desirability function value close to 1. Figure 1 shows the optimized SLN formulation demarcated in the design space overlay plot, which specified the composition of Capmul MCM C10 (275 mg), poloxamer (165 mg), soy lecithin (55 mg), homogenization speed at 8000 rpm and stirring speed at 1750 rpm. The overlay plot indicated that predicted values of the responses, where particle size of 88.54 nm, entrapment efficiency of 66% and loading capacity of 11.53% were observed.

Supplementary data Table 2A-C shows the validation of experimental methodology perfumed by developing the check-point formulation trials, which revealed close similarity of the predicted responses with the observed ones by high magnitude of R and correlation plots ranging between 0.948 and 0.972 ($P < 0.0001$). Moreover, the corresponding residual plots narrow, randomized and uniform distribution of the around the zero axis. Figure 2(A, B) shows the particle size distribution of the optimized GA-SLN as 73 nm with polydispersity index value of 0.159, while Fig. 2C and D portray the images of field emission scanning electron microscopy and transmission electron microscopy (TEM) of the optimized GA-SLNs in nanosized structure and spherical shape appearance.

In Vitro Drug Release Studies

Figure 3 shows the SLN formulations in vitro drug release profiles of the optimized GA-SLNs and GA solution. Different drug release characteristics has been observed from these formulations with the maximum drug release (i.e. > 70%) was observed within first 8-h time period. Further, the data

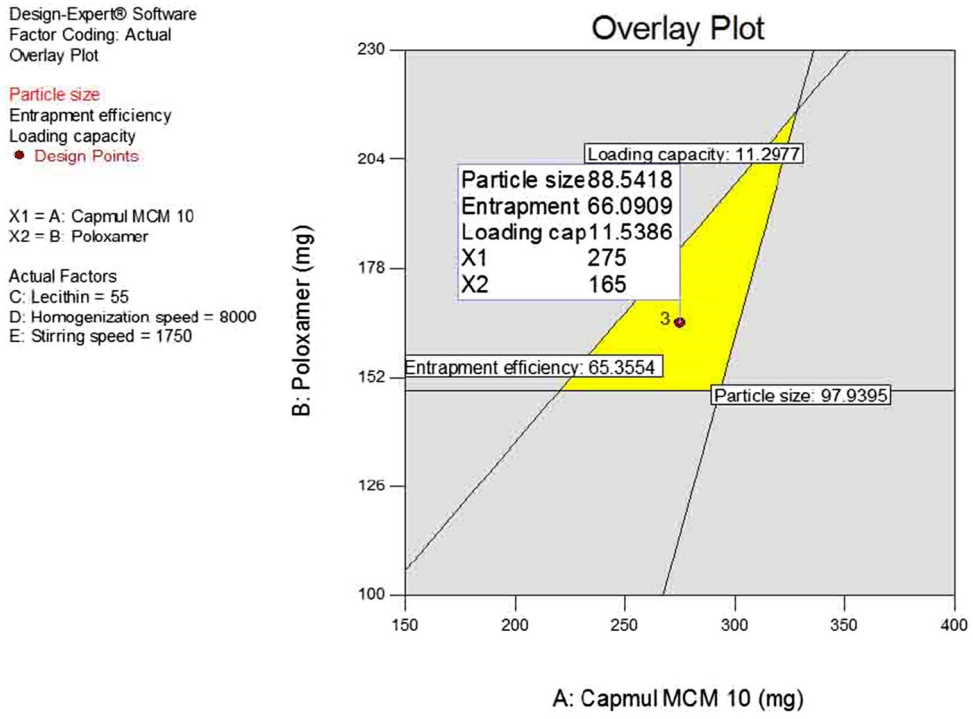

Fig. 1 Overlay plot obtained from graphical optimization, indicating yellow region as design space and flagged point as the optimized GA-loaded solid lipid nanoparticles

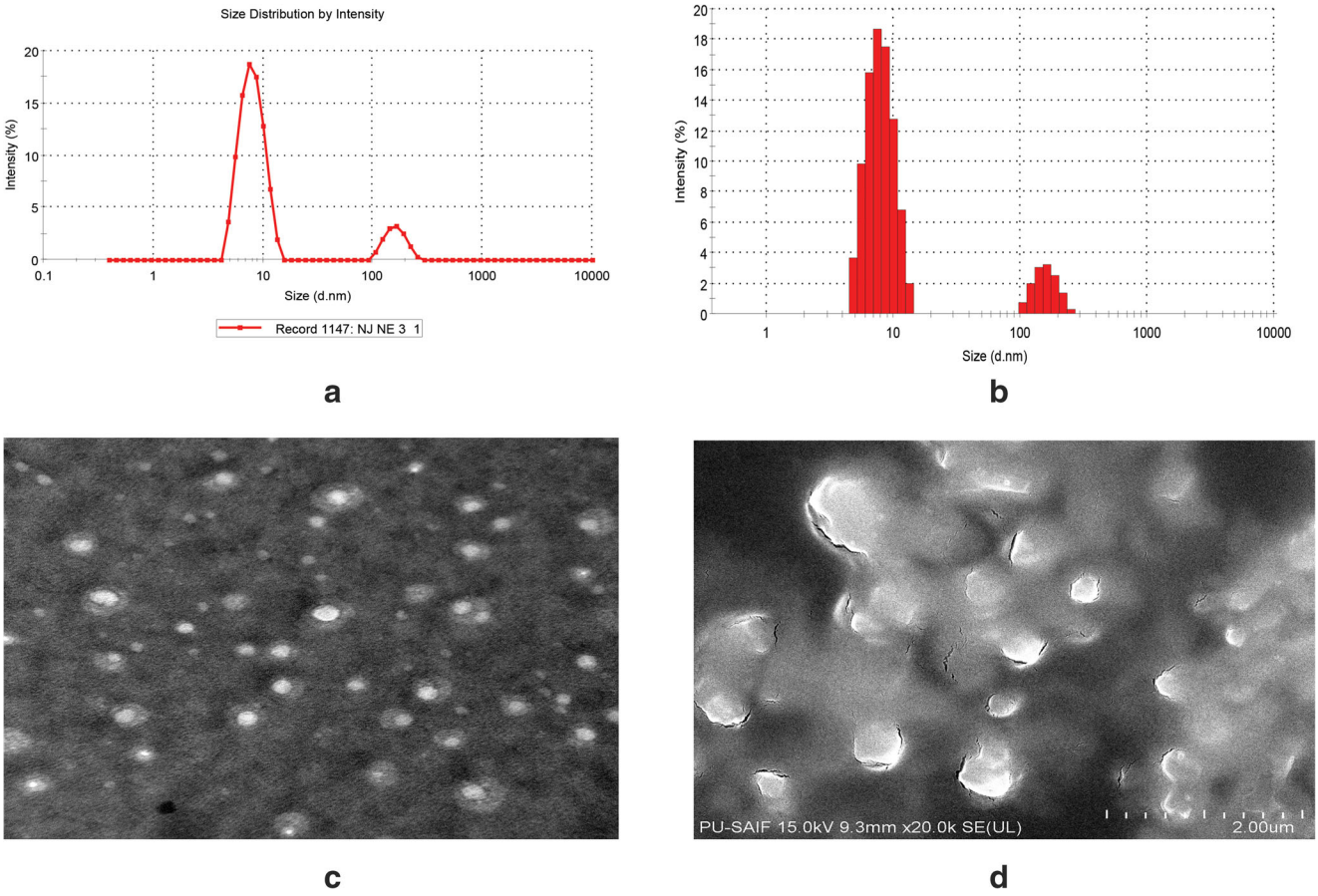

Fig. 2 (A–D) Characterization of optimized GA-SLN: (A–B) shows particle size distribution curve (C) TEM analysis and (D) FE-SEM

indicated that GA release from the SLNs exhibited a biphasic pattern of drug release within 4 h, while the remaining amount of drug release was observed within next 8 h. The mathematical modelling of the release data from GA-SLN followed first-order release kinetics exhibiting R value of 0.9756. Besides, Korsmeyer-Peppas model applied to the drug release data indicated the value of release exponent (n) for the optimized SLN is 0.846, thus indicated drug release via anomalous (non-Fickian) diffusion mechanism. The observed results are inconsonance with the previously published literature reports on several reports [18, 20, 22].

In Vitro Cytotoxic Activity

The MTT assay results of GA solution, GA-SLNs and plain SLNs on HepG2 cells for 24- and 48- and 72-h time periods are shown in Fig. 4(A–C). The data indicated cell viability of formulation at the different drug concentrations, where reduction

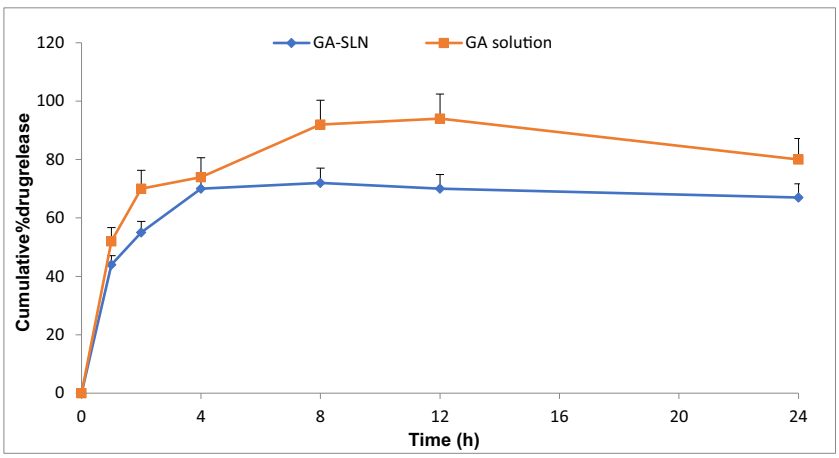

Fig. 3 In vitro release of ganoderic acid–loaded solid lipid nanoparticles (GA-SLN) and GA solution at different time intervals (0–24 h) using the dialysis method in simulated intestinal fluid of pH 6.8

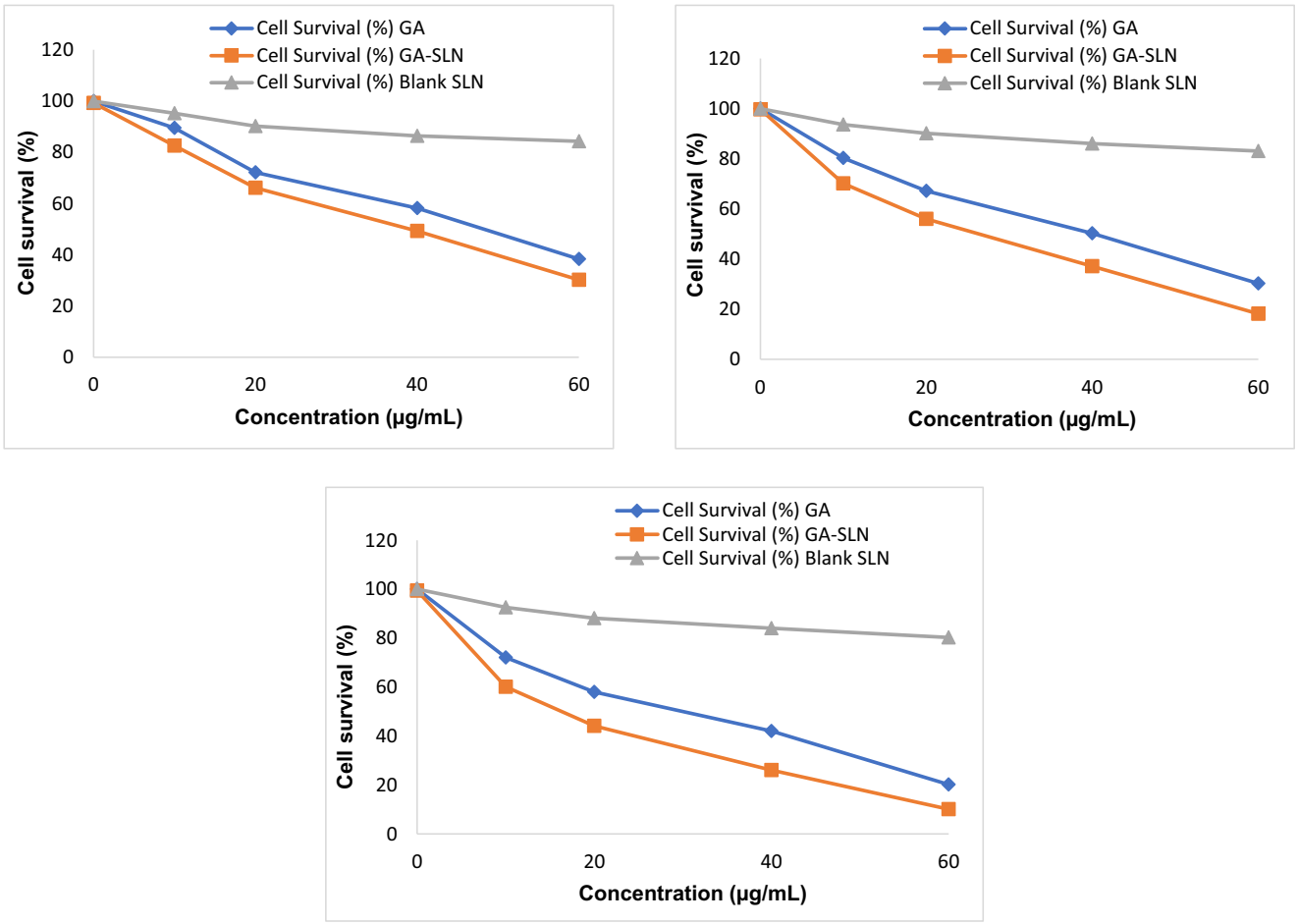

Fig. 4 (A–C) Assessment of cell viability of GA solution, GA-SLN and Blank SLN formulation at different concentration following incubation with HepG2 cells, (A) for 24 h, (B) for 48 h, and (C) for 72 h duration

in the cell viability was found to be dependent on the concentration of drug. Therefore, the results concluded that maximal reduction in cell viability on HepG2 cell line was due to GA-SLNs over GA solution only. In addition, GA-SLN showed maximal reduction in cell viability up to 72 h at lower values of IC_{50} (as shown in Table 1).

Sterilization and Stability Studies

Sterilization of the SLNs containing poloxamer 188 was not possible by autoclaving due to reduced steric stabilization of the surfactant at increased temperature close to the CFT [25]. Alternatively, the sterilization by filtration or gamma irradiation was performed. In this regard, the nanoparticles were sterilized by passing through 0.22-µm membrane filters. When GA-SLNs were passed through the membrane filter, the mean particle size remained unchanged.

Table 1 MTT viability assay of GA solution and optimized GA-SLN. The GA-SLN shows significant ($P < 0.05$) cytotoxicity compared with GA solution after 24 h, 48 h and 72 h. Data are expressed as mean ± SD ($n = 6$)

Formulations	IC_{50} (µg/mL)		
	24 h	48 h	72 h
GA solution	45.123	39.112	36.211
GA-SLN	37.201	30.510	25.101

IC_{50}, half maximal inhibitory concentration

Table 2 Particle size, size distribution, entrapment efficiency and loading of SLN following storage at 25 °C/60% RH

Time (in weeks)	Particle size	PDI	EE (%)	LC (%)
0	73 nm	0.159	66	11.5
1	71.1 nm	0.134	65.9	11.3
2	69.2 nm	0. 18	65.7	11.1
4	68.31 nm	0. 21	65.4	11
8	66.21 nm	0.25	65.1	10.9
12	66.11 nm	0. 27	64.8	10.9

PDI, polydispersity index; *EE*, entrapment efficiency; *LC*, loading capacity; *SLN*, solid lipid nanoparticles

Table 3 Particle size, size distribution, entrapment efficiency and loading of SLN following storage at 40 °C/75% RH

Time (in weeks)	Particle size	PDI	EE (%)	LC (%)
0	73 nm	0.158	66	11.5
1	75 nm	0.161	64.21	11.1
2	76 nm	0.263	60.13	10.8
4	84 nm	0.383	57.12	10.6
8	110.21 nm	0.494	55.34	10.2
12	135.7 nm	0.698	52	10.0

Particle Size Distribution and Polydispersity Index

The particle size (PS) of the optimized GA-SLN stored at 25 °C/60% and 40 °C/75% RH ranged between 73 to 66.11 nm and 73 to 135.7 nm, respectively (shown in Tables 2 and 3). The PS of SLNs was quite unchanged during storage at 25 °C/60% RH, while at 40 °C/75% RH, the particle size was increased due to the aggregation phenomenon occurs due to increase in kinetic energy of the system [26]. However, the polydispersity index (PDI) data revealed low and constant values, thus confirming physically stable nature of the PS during storage at 25 °C/60% RH for at least 12 weeks (as shown in Table 2).

Encapsulation Efficiency and Loading Capacity

The encapsulation efficiency (EE) of the optimized GA-SLN at 25 °C/60% RH ranged from 66 to 64.8%, whereas the loading capacity (LC) ranged from 11.5 to 10.9%. The EE of said formulation at 40 °C/75% RH ranged from 66 to 52%, and LC ranged from 11.5 to 10% (data shown in Tables 2 and 3). Moreover, the amount of GA entrapped in SLNs remained constant or nonsignificant over 12 weeks of storage at 25 °C/60% RH. However, at storage temperature of 40 °C/75% RH, the EE and LC of the said formulation revealed a significant decrease that can be correlated to the polymorphic forms of the lipid [26].

Effect of GA-SLNs on the Macroscopic Structure

Macroscopically no hepatic nodules were found in a normal and normal control group (Fig. 5A) treated with GA (1000 mg/kg), whereas white hepatic nodules distributed on the liver and uneven cirrhosis were found in the groups treated with DEN. In DEN-induced HCC rats treated with GA (25 mg/kg and 100 mg/kg), white hepatic nodules and blood vessel decreased relative to DEN-induced HCC rats and white nodules in GA-SLN (25 mg/kg) disappear entirely (Fig. 5B–D). In another group of DENA-induced HCC rats who received GA at the dose of 100 mg/kg of GA solution and GA-SLN, 3 out of 7 rats and 2 out of 8 showed hepatic nodules only, as shown in Tables 4 and 5.

Tables 2 and 3 represent a total of 245 number of hepatic nodules induced by the DEN group rats with dimensions of ≤ 1 mm (117), < 3 mm > 1 mm (69) and ≥ 3 mm (59), respectively. DEN-induced GA treatment group of rats showed 66.6, 42.85% of hepatic nodules and the size of ≤ 1 mm (82, and 72), < 3 mm > 1 mm (52 and 45) and ≥ 3 mm (31, and 25) at a dose of 25 and 100 mg/kg respectively. On the other hand, 25% of hepatic nodule occurrence with a size of GA-SLN (25 mg/kg) treatment rats showed size ≤ 1 mm (40), < 3 mm > 1 mm (35) and ≥ 3 mm (6), respectively (shown in Tables 4 and 5).

Animal Weight and Liver Weight

The body and liver weight of all the group of rats are illustrated in Fig. 6A and B. GA (100 mg/kg) used in NC and NC rats at the end of the study, showing an increased body weight. The group of rats induced from DEN has shown a substantial reduction ($P < 0.001$) in body weight relative to body weight. Overall, the body weight was not increased as compared with NC and NC received GA (100 mg/kg). DEN-induced rats treated with GA (25 and 100 mg/kg) showed the significant ($P < 0.001$) body weight increase in comparison with DEN-induced group rats. GA-SLN-treated rats showed the enhanced body weight effect, which was increased almost near

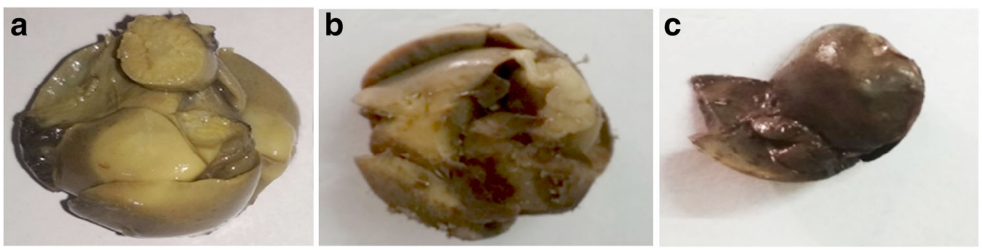

Fig. 5 (A–C) Macroscopical observation of DEN-induced HCC group rats. (A) DEN control group showed the expansion of hepatic nodules (while in colour) and decolourization of tissue; (B) DEN control group treated with GA (25 mg/kg) illustrated the expansion of pre-cancerous nodules (white in colour) and decolourization of tissue colour, which was less as compared with DEN group; (C) DEN control group treated with GA-SLN (25 mg/kg) illustrated the decolourization of tissue colour, which was very less as compared with other group rats). Note: Normal control rats not found any sign of alteration (data not shown)

Table 4 The effect of GA-SLN on the number of rats, number of nodules and average number of nodules bearing rats

S. No.	Groups	Number of rats with nodules/number of rats	Total number of nodules	Relative size (% of number size)		
				≤ 1 mm	< 3 mm > 1 mm	≥ 3 mm
1	Normal control	6/6	0	0	0	0
2	DENA control	9/9	202	117	69	59
3	DENA+GA (25 mg/kg)	5/9	160	82	52	31
4	DENA+GA (100 mg/kg)	3/7	142	72	45	25
5	DENA+GA-SLN (25 mg/kg)	2/8	81	40	35	6

Group I and group VI did not show any sign of hepatic nodules

Table 5 GA-SLN, its effects on number of rats with tumour incidence

S. No.	Groups	Number of rats/number of rats with tumour	Tumour incidence (%)
1	Normal control	6/6	0
2	DENA control	9/9	100
3	DENA+GA (25 mg/kg)	5/9	66.6
4	DENA+GA (100 mg/kg)	3/7	42.85
5	DENA+GA-SLN (25 mg/kg)	2/8	25

Group I and group VI did not show any sign of hepatic nodules

to NC group rats. An opposite trend was observed in the hepatic tissue, NC and NC received GA (100 mg/kg) showed almost similar liver weight (Figure 6n). The enhanced liver weight was shown by DEN-induced rats up to 1.5-times higher than the NC group rats. The reduced liver weight in contrast with DEN group rats was shown in DEN-induced rats treated with GA (25, 100 and 100 mg/kg). GA-SLN (25 mg/kg)-treated rats found the reduced liver weight, which was significant ($P < 0.001$) to reach near NC group rats (as shown in Fig. 6B).

Evaluation of Antioxidant Markers

The levels of LPO (13.08 ± 1.59) were enhanced in the DEN control group and significantly ($P < 0.01$) higher and make normalized after administration of GA, i.e. (8.79 ± 0.88) at a dose of 100 mg/kg. Furthermore, GA-SLNs significantly cause lowering of LPO value (7.45 ± 0.91), at the dose of 25 mg/kg which is showed in Table 6. Apart from above, reduction in enzymatic level of CAT (0.05 ± 0.52),SOD (0.99 ± 0.81), GPX (4.98 ± 0.65), GST (0.04 ± 0.13) was found in the DEN control group, whereas GA showed enhancement of CAT (0.89 ± 0.16), SOD (1.85 ± 0.71), GPX (7.34 ± 0.56) and GST (0.49 ± 0.71). Further, GA-SLN (25 mg/kg) made more increment in the value of antioxidants enzymes including CAT (0.99 ± 0.31), SOD (2.01 ± 0.51), GPX (8.02 ± 0.61) and GST (0.55 ± 0.42) and approached to the normal value as to normal control (as shown in Table 6). Antioxidants play an important part in different biological activities, including reducing, reversing the carcinogenic impact and free radicals [27, 28]. Antioxidants inhibited ROS primarily by regulating the development of ROS and freeing the oxidative stress. DEN administration causes increased oxidative stress because free radicals over-produced through lipid peroxidation during HCC [27, 28]. Various pathological conditions are directly concerning to the lipid peroxidation.

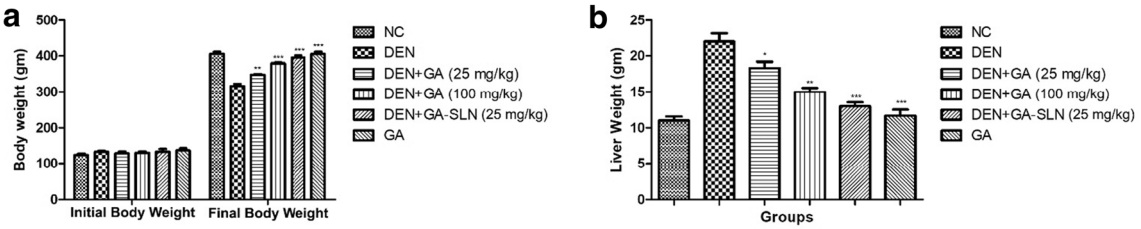

Fig. 6 (A, B) The body effect of GA and GA-SLN treatment on the DEN-induced HCC rats. (A) shows the body weight of different group of rats; (B) demonstrates the liver tissue weight of different group of rats

Table 6 The effect on the antioxidant parameters of GA and GA-SLN treatment on the DEN-induced HCC rats

Group	LPO (μM/mg protein)	CAT (nmol/min/ml)	SOD (U/ml)	GPx (μmol)	GST (U/min/mg protein)
Normal control	7.11 ± 0.71	1.25 ± 0.68	2.07 ± 0.40	8.14 ± 0.79	0.60 ± 0.03
DENA control	13.08 ± 1.59[a]	0.05 ± 0.52[a]	0.99 ± 0.81[a]	4.98 ± 0.65[a]	0.04 ± 0.13[a]
DENA+GA (25 mg/kg)	9.61 ± 1.04**	0.86 ± 0.08**	1.35 ± 0.50**	7.06 ± 0.28**	0.40 ± 0.45**
DENA+GA (100 mg/kg)	8.79 ± 0.88**	0.89 ± 0.16**	1.85 ± 0.71**	7.34 ± 0.56**	0.49 ± 0.71**
DENA+GA-SLN (25 mg/kg)	7. 45 ± 0.91**	0.99 ± 0.31**	2.01 ± 0.51**	8.02 ± 0.61**	0.55 ± 0.42**
GA only	7.22 ± 1.40**	0.45 ± 0.41*	1.49 ± 0.10*	6.32 ± 0.52*	0. 21 ± 0.32**

Values are expressed as mean ± SEM. ($n = 6$). Statistical significance $P < 0.05$

[a] $P < 0.001$ as compared with normal group

*$P < 0.01$ as compared with DENA treated group

**$P < 0.001$ as compared with DENA treated group

Thus, accurate determination of lipid peroxidation (LPO) can mark the accurate redox state of cells and induces the damage to cellular macromolecules by ROS production [28]. The findings of DEN-inducing HCC lead to an enhanced LPO rate, an important indication of imbalance in redox cell state and oxidative stress [11, 22, 27, 28]. CAT and SOD are the first-generation defence endogenous proteins of antioxidant antioxidants. GA-SLN ($P < 0.001$) considerably decreases LPO material and avoids lipid peroxidation, owing to the powerful antioxidants impact of GA, which prevents the oxidation. SOD have primary function is to reduce the superoxide's, which is generated during oxidative phosphorylation as a by-product to hydrogen peroxide radical and water [22, 28–30], whereas CAT or GPx play a key role in the conversion of H_2O_2 to H_2O [27, 28]. DEN-induced HCC have remarkable lowering of these enzymes, resulted to increased production of free radical and make depletion of endogenous redox system. Another way is DEN, an electrophilic carcinogen which interacts with nucleophilic sites of GSH resulted to macromolecules interaction. GSH plays a major role in preserving reduced cell state by removing free radicals [31–33]. With the therapeutic strategy, GA-SLN administration in DEN-induced HCC rats quickly enhanced levels of GSH relative to DEN and altered the favourable carcinogenesis. Other antioxidants like SOD, CAT, GSH and GPx were decreased in DEN-induced rats, due to growth of tumour. In a nutshell, GA-SLNs acted like endogenous antioxidants and scavengers of the excessive free radicals to produce the protective effects.

Conclusions

The present study revealed development of the optimized GA-SLNs which exhibited satisfactory particle size distribution, entrapment efficiency, loading capacity and in vitro drug release characteristics. Besides, cell cytotoxicity and antitumor activity evaluation study confirmed enhanced anticancer activity of the GA-SLNs as compared with the GA solution. From this study, it can be concluded the success of nano-antioxidant therapy to be highly effective against HCC treatment.

Compliance with Ethical Standards

Experiments were conducted as per the guidelines issued by all the international guidances as well as the guidelines of Committee for Protection, Control and Supervision on Experimental Animals (CPCSEA), Govt. of India. The study protocol was approved by the Institutional Animal Ethical Committee (IAEC) of Siddhartha Institute of Pharmacy, Dehradun, India (Reg. No. SIP/IAEC/PCOL/06/2017). In addition, all laboratory parameters linked to animals were performed in accordance with the appropriate IAEC rules and laws.

Conflict of Interest The authors declare that they have no conflict of interest.

References

1. Lawrence TS, Robertson JM, Anscher MS, et al. Hepatic toxicity resulting from cancer treatment. Int J Radiat Oncol Biol Phys. 1995;1:1237–48.
2. Perz JF, Armstrong GL, Farrington LA, Hutin YJF, Bell BP. The contributions of hepatitis B virus and hepatitis C virus infections to cirrhosis and primary liver cancer worldwide. J Hepatol. 2006;45:529–38.
3. Bosch FX, Ribes J, Díaz M, Cléries R. Primary liver cancer: worldwide incidence and trends. Gastroenterology. 2004;127:S5–S16.
4. Anwar F, Gohar M, Kazmi I, et al. Anticancer effect of rosiglitazone in rats treated with N-nitrosodiethylamine via inhibition of DNA synthesis: an implication for hepatocellular carcinoma. RSC Adv. 2015;5:68385–91.
5. Raza A, Sood GK. Hepatocellular carcinoma review: current treatment, and evidence-based medicine. World J Gastroenterol. 2014;20:4115–27.
6. Bishop KS, Kao CH, Xu Y, et al. From 2000 years of Ganoderma lucidum to recent developments in nutraceuticals. Phytochemistry. 2015;114:56–65.
7. Kang MH, Reynolds CP. Bcl-2 inhibitors: targeting mitochondrial apoptotic pathways in cancer therapy. Clin Cancer Res. 2009;15:1126–32.

8. Pandey P, Rahman M, Bhatt PC, Beg S, Paul B, Hafeez A, et al. Implication of nano-antioxidant therapy for treatment of hepatocellular carcinoma using PLGA nanoparticles of rutin. Nanomedicine (London). 2018;13:849–70.
9. Lin Z, Zhang H. Anti-tumor and immunoregulatory activities of Ganoderma lucidum and its possible mechanisms. Acta Pharmacol Sin. 2004;25:1387–95.
10. Boh B, Berovic M, Zhang J, et al. Ganoderma lucidum and its pharmaceutically active compounds. Biotechnol Annu Rev. 2007;13:265–301.
11. Kimura Y, Taniguchi M, Baba K. Antitumor and antimetastatic effects on liver of triterpenoid fractions of Ganoderma lucidum: mechanism of action and isolation of an active substance. Anticancer Res. 2002;22:3309–18.
12. Beg S, Hasnain MS. Pharmaceutical Quality by Design: principles and applications. New York: Academic Press (Elsevier); 2019.
13. Beg S, Rahman M, Kohli K. Quality-by-design approach as a systematic tool for the development of nanopharmaceutical products. Drug Discov Today. 2019;24:717–25.
14. Beg S, Rahman M, Panda SS. Pharmaceutical QbD: omnipresence in the product development lifecycle. Eur Pharm Rev. 2017;22:58–64.
15. Beg S, Akhter S, Rahman M, Rahman Z. Perspectives of Quality by Design approach in nanomedicines development. CurrNanomed. 2017;7:191–7.
16. Beg S, Saini S, Bandopadhyay S, Katare OP, Singh B. QbD-driven development and evaluation of nanostructured lipid carriers (NLCs) of olmesartanmedoxomil employing multivariate statistical techniques. Drug Dev Ind Pharm. 2018;44:407–20.
17. Khurana RK, Bansal AK, Beg S, Burrow AJ, Katare OP, Singh KK, et al. Enhancing biopharmaceutical attributes of phospholipid complex-loaded nanostructured lipidic carriers of mangiferin: systematic development, characterization and evaluation. Int J Pharm. 2017;518:289–306.
18. Beg S, Jain S, Kushwah V, Bhatti GK, Sandhu PS, Katare OP, et al. Novel surface-engineered solid lipid nanoparticles of rosuvastatin calcium for low-density lipoprotein-receptor targeting: a Quality by Design-driven perspective. Nanomedicine (London). 2017;12:333–56.
19. Ekambaram P, Abdul HAS. Formulation and evaluation of solid lipid nanoparticles of ramipril. J Young Pharm. 2011;3:216–20.
20. Beg S, Alam MN, Ahmad FJ, Singh B. Chylomicron mimicking nano-colloidal carriers of rosuvastatin calcium for lymphatic drug targeting and management of hyperlipidemia. Colloids Surf B: Biointerfaces. 2019;177:541–9.
21. Harshita, Barkat MA, Rizwanullah M, Beg S, Pottoo FH, Siddiqui S, et al. Paclitaxel-loaded nanolipidic carriers with improved oral bioavailability and anticancer activity against human liver carcinoma. AAPS PharmSciTech. 2019;20:87.
22. Rahman M, Abdullah SA, Alharbi KS, Beg S, Sharma K, Anwar F, et al. Ganoderic acid loaded nano-lipidic carriers improvise treatment of hepatocellular carcinoma. Drug Deliv. 2019;26:629–40.
23. Shafique H, Ahad A, Khan W, Want MY, Bhatt PC, Ahmad S, et al. Ganoderic acid-loaded solid lipid nanoparticles ameliorate d-galactosamine induced hepatotoxicity in Wistar rats. J Drug Deliv Sci Technol. 2019;50:48–56.
24. Beg S, Sharma G, Thanki K, Jain S, Katare OP, Singh B. Positively charged self-nanoemulsifying oily formulations of olmesartanmedoxomil: systematic development, in vitro, ex vivo and in vivo evaluation. Int J Pharm. 2015;493:466–82.
25. Nayak AP, Tiyaboonchai W, Patankar S, Madhusudhan B, Souto EB. Curcuminoids-loaded lipid nanoparticles: novel approach towards malaria treatment. Colloids Surf B: Biointerfaces. 2010;81:263–73.
26. Uner M. Preparation, characterization and physico-chemical properties of solid lipid nanoparticles (SLN) and nanostructured lipid carriers (NLC): their benefits as colloidal drug carrier systems. Pharmazie. 2006;61:375–86.
27. Kim WR, Flamm SL, Bisceglie D, et al. Serum activity of alanine aminotransferase (ALT) as an indicator of health and disease. Hepatology. 2008;47:1363–70.
28. Jain AK, Thanki K, Jain S. Novel self-nanoemulsifying formulation of quercetin: implications of pro-oxidant activity on the anticancer efficacy. Nanomed Nanotechnol Biol Med. 2014;10:959–69.
29. Kumar V, Bhatt PC, Rahman M, Kaithwas G, Choudhry H, al-Abbasi F, et al. Fabrication, optimization, and characterization of umbelliferone β-D-galactopyranoside-loaded PLGA nanoparticles in treatment of hepatocellular carcinoma: in vitro and in vivo studies. Int J Nanomedicine. 2017;12:6747–58.
30. Joshi BC, Prakash A, Kalia AN. Hepatoprotective potential of antioxidant potent fraction from *Urticadioica* Linn. (whole plant) in CCl_4 challenged rats. Toxicol Rep. 2015;2:1101–10.
31. Prasad L, Khan TH, Jahangir T, Sultana S. Abrogation of DEN/Fe-NTA induced carcinogenic response, oxidative damage and subsequent cell proliferation response by Terminalia chebula in kidney of Wistar rats. Pharmazie. 2007;62:790–7.
32. Khan R, Kazmi I, Afzal M, al Abbasi FA, Mushtaq G, Ahmad A, et al. Fixed dose combination therapy loperamide and niacin ameliorates diethylnitrosamine-induced liver carcinogenesis in albino Wistar rats. RSC Adv. 2015;5:67996–8002.
33. Verma A, Singh D, Anwar F, Bhatt PC, al-Abbasi F, Kumar V. Triterpenoids principle of Wedelia calendulacea attenuated diethynitrosamine-induced hepatocellular carcinoma via down-regulating oxidative stress, inflammation and pathology via NF-kB pathway. Inflammopharmacology. 2018;26:133–46.